Stimulus driver for epilepsy seizure suppression with adaptive loading impedance



2011 J. Neural Eng. 8 066008

(http://iopscience.iop.org/1741-2552/8/6/066008)

J. Neural Eng. **8** (2011) 066008 (7pp) doi:10.1088/1741-2560/8/6/066008

# Stimulus driver for epilepsy seizure suppression with adaptive loading impedance

**Ming-Dou Ker, Chun-Yu Lin and Wei-Ling Chen**

Nanoelectronics and Gigascale Systems Laboratory, Institute of Electronics, National Chiao-Tung University, 1001 University Road, Hsinchu, Taiwan

E-mail: mdker@ieee.org

Received 18 June 2011
Accepted for publication 27 September 2011
Published 26 October 2011
Online at stacks.iop.org/JNE/8/066008

**Abstract**

A stimulus driver circuit for a micro-stimulator used in an implantable device is presented in this paper. For epileptic seizure control, the target of the driver was to output 30 $\mu$A stimulus currents when the electrode impedance varied between 20 and 200 k$\Omega$. The driver, which consisted of the output stage, control block and adaptor, was integrated in a single chip. The averaged power consumption of the stimulus driver was 0.24–0.56 mW at 800 Hz stimulation rate. Fabricated in a 0.35 $\mu$m 3.3 V/24 V CMOS process and applied to a closed-loop epileptic seizure monitoring and controlling system, the proposed design has been successfully verified in the experimental results of Long-Evans rats with epileptic seizures.

(Some figures in this article are in colour only in the electronic version)

## 1. Introduction

Epilepsy, caused by abnormal discharge activity in the brain, is one of the most common neurological disorders and seriously restrains patient's daily life. In an epidemiological study in a northern county of Sweden, there were 70 patients with epileptic seizures in a population consisting of 52 252 children aged 0–15 years [1]. In other words, the incidence rates of epileptic seizures were estimated to be 134/100 000. Millions of people suffer from epilepsy in the world. As medical science is improving continuously, therapies of epileptic seizure include pharmacologic treatment and surgical treatment. Most patients can be ameliorated by antiepileptic drugs (AEDs); however, every kind of such medicines might lead to side effects including blurry vision, dizziness, headache and fatigue [2, 3]. Besides, some patients do not respond to AEDs. Their epilepsy is medically refractory. For patients who do not respond to medicament, non-reversible brain surgery is commonly used. This is risky surgery that may cause functional losses. Besides, not all patients respond well to traditional therapies [4].

As medical science and electronics engineering have evolved, bioelectronics combining microelectronics technology with medical knowledge results in a new generation of healthcare and therapy. There are several fabulous applications of bioelectronics such as magnetic resonance imaging and electroencephalography (EEG). In recent decades, the inseparable relationship between electrical transaction and nervous system has been studied [5]. Thus, therapeutic electrical stimulation (TES) that transmits artificial electrical signals into the nervous system has been verified for innovative medical treatments in different applications, such as cardiac pacing, muscle exercising and vision restoration [6, 7]. Currently, electrical treatment for epilepsy is also being reported [8, 9].

The predictability of epileptic seizures has been studied by analyzing EEG in time or frequency domains [10]. Although the possibility of seizure prediction remains to be clarified [11], several methods of prediction have been researched, such as predictive features and prediction by classification [12, 13]. It has also been demonstrated that the abnormal discharge signal that causes epileptic seizure can be suppressed by TES before the seizure occurs [14]. Compared to non-reversible surgery, electrical stimulation treatment is more harmless to tissue in the brain and more flexible. Therefore, TES is a possible way to suppress epileptic seizure or cure other

 

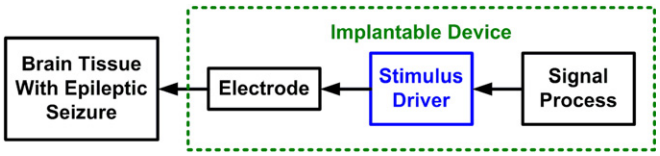


**Figure 1.** The block diagram of the implantable stimulus driver for epileptic treatment.

diseases. However, the stimulus driver for TES still faces several challenges. Due to different kinds of tissues, location and implanted time, the effective impedance of the electrode varies in a wide range. The impedance ranges from tens of kΩ to several hundreds of kΩ [15]. Under this condition, while the required stimulus current is fixed, the output voltage varies correspondingly in a wide range. High operating voltage might result in problems of gate-oxide reliability and hot-carrier effect [16]. In addition, power consumption is also the critical consideration, because it is inversely proportional to the used time of the implantable device. Recently, some power-efficient neural stimulators with constant current stimulation have been presented [17, 18].

However, the stimulus driver that considers the power consumption, reliability, safety and adaptive loading impedance was never reported in the literature. In this work, a new implantable stimulus driver for epileptic seizure suppression with above-mentioned considerations is proposed. Figure 1 shows the block diagram of the implantable stimulus driver for epileptic treatment. The detailed circuit design and measurement results of the proposed design are presented in the following sections.

## 2. New design of the stimulus driver

### 2.1. CMOS process

The required stimulus current is 30 $\mu$A in this work, and the effective electrode impedance varies from 20 to 200 kΩ. In order to meet the requirements, the range of the stimulus voltage should be kept from 0.6 to 6 V. Therefore, a 0.35 $\mu$m 3.3 V/24 V CMOS process is used for chip implementation. The process includes the low voltage part of 3.3 V logic devices and the high voltage part which can reach up to 24 V. The proposed stimulus driver will not suffer from the problems of gate-oxide reliability and hot-carrier degradation which might lead to failure of the implantable stimulus driver.

### 2.2. Circuit implementation

The proposed stimulus driver consisting of the output stage, control block and adaptor is shown in figure 2 [19]. This circuit was designed for monophasic stimulation with 800 Hz, 40% duty cycle and 30 $\mu$A pulse train for 0.5 s [15]. However, it can be easily expanded to a biphasic one. The output stage is implemented with 24 V devices. Besides, in order to reduce the size of the device and power consumption, the control block and adaptor adopt the 3.3 V devices with a fixed operating voltage ($V_{DD}$).

For safety consideration, the blocking capacitor of the output stage in series with the tissue serves an important purpose: to prevent prolonged dc current from flowing into the tissue in the event of semiconductor failure [20]. However, in order to output the stimulus current with the required duration and amplitude, the size of the blocking capacitor would be too large to be integrated into a chip. For stimulation with 30 $\mu$A current and 0.5 ms duration on the 20 kΩ electrode

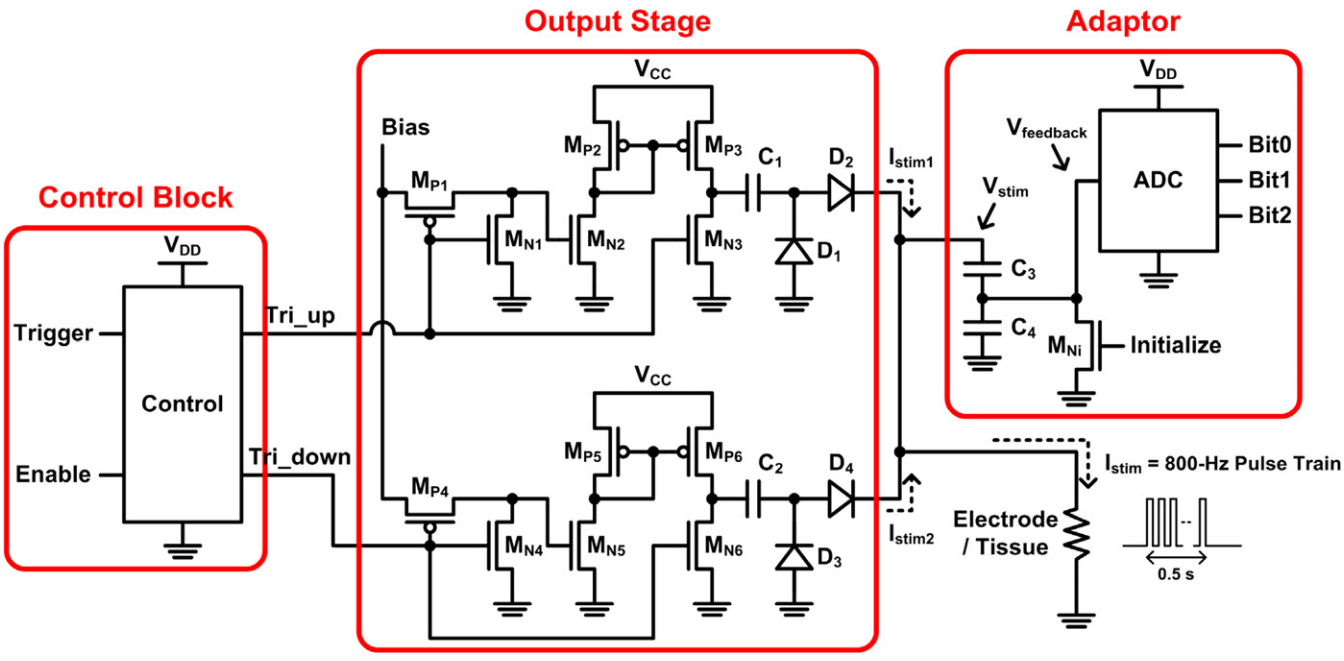


**Figure 2.** The proposed stimulus driver consisting of the output stage with blocking capacitors, control block and adaptor.

impedance, the required blocking capacitance is ∼0.2 $\mu$F to keep the stimulus current within 10% variation. In order to solve the problem of a large-sized blocking capacitor, the high-frequency current-switching blocking capacitor has been studied to reduce the size of the blocking capacitor [21]. For a given stimulus current ($I_{stim}$), both the reduction of pulse duration (d$t$) and the increase of voltage drop (d$V$) across the blocking capacitor can reduce the required size of the capacitor. The technique of the high-frequency current-switching blocking capacitor utilizes two complementary current sources with blocking capacitors. Complementary stimulus current outputs ($I_{stim1}$ and $I_{stim2}$) converge and form a complete stimulus current ($I_{stim}$, which is the sum of $I_{stim1}$ and $I_{stim2}$). Thus, each stimulus duration is reduced, while current amplitude and voltage drop are not changed. The reduction ratio of the blocking capacitor is directly proportional to switching frequency. By adopting the technique of the high-frequency current-switching blocking capacitor with 2.5 MHz switching frequency, only ∼0.1 nF capacitor is required to deliver 30 $\mu$A stimulus current within 200 ns duration.

In this work, for the purpose of reducing the size of the blocking capacitor and minimizing the voltage drop on the blocking capacitor, the switching frequency is set as 2.5 MHz. The 2.5 MHz frequency can be obtained from the clock signal of the signal process part in the implantable device. As shown in figure 2, the output stage of the proposed stimulus driver adopts the high-frequency current-switching blocking capacitor. During the 'turn-on' interval of the stimulus driver, the control signals of Trigger, Tri_up and Tri_down switch complementarily. During the upper stimulating phase, Tri_up is low (0 V) and Tri_down is high (3.3 V). For the upper current source, $M_{N2}$ is biased through $M_{P1}$, and $M_{N3}$ is switched off. The stimulus current is delivered by current mirrors $M_{P2}$ and $M_{P3}$, and passes through $C_1$ and $D_2$. Meanwhile, the down current source is in the discharging phase, $M_{N5}$ is switched off and $M_{N6}$ is switched on. The charged $C_2$ can be discharged by $M_{N6}$ and $D_3$. During the down stimulating phase, Tri_up is high (3.3 V) and Tri_down is low (0 V). For the upper current source, $M_{N2}$ is switched off and $M_{N3}$ is switched on. The charged $C_1$ can be discharged by $M_{N3}$ and $D_1$. Meanwhile, the down current source is in the stimulating phase, stimulus current is delivered by current mirrors $M_{P5}$ and $M_{P6}$, and passes through $C_2$ and $D_4$. During the 'turn-off' interval of the stimulus driver, both Tri_up and Tri_down are high (3.3 V), gates of $M_{N2}$ and $M_{N5}$ are low (0 V), and no stimulus current is delivered. According to the structure of the proposed stimulus driver, the required operating voltage ($V_{CC}$) of the output stage is shown by

$$V_{CC(min)} = V_{ds,P} + \Delta V_C + \Delta V_{diode} + R_{electrode} \times I_{stim}, \quad (1)$$

where $V_{ds,P}$ denotes the voltage drop between the drain and source terminals of $M_{P3}$ or $M_{P6}$, $\Delta V_C$ denotes the voltage drop across $C_1$ or $C_2$, and $\Delta V_{diode}$ is the voltage drop across $D_2$ or $D_4$. It is obvious that $V_{CC}$ can be adjusted according to the electrode impedance ($R_{electrode}$) and stimulus current ($I_{stim}$). In addition, the electrode impedance and stimulus current in equation (1) usually dominate the required $V_{CC}$. Thus, if the electrode impedance varies largely, the required $V_{CC}$ will also be changed.

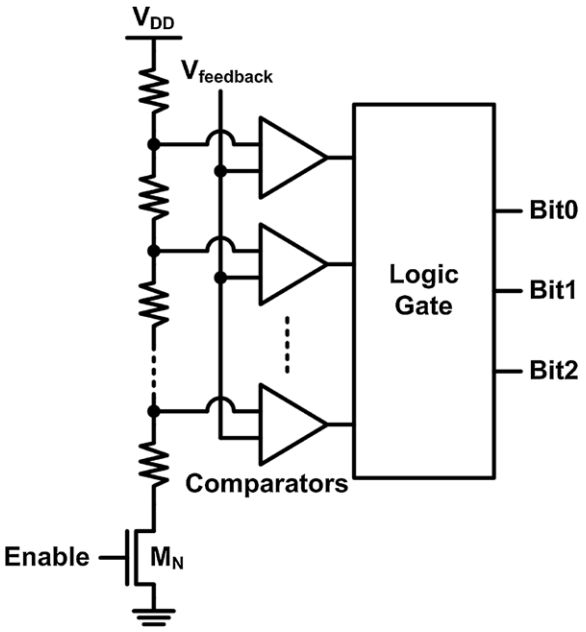


**Figure 3.** The 3-bit ADC used in the adaptor to detect the stimulus voltage.

Under the condition that the required seizure suppressing stimulus current is 30 $\mu$A and the electrode impedance varies from 25 to 200 kΩ, the difference of the required operating voltages is ∼6 V. Conventional stimulus drivers often use the operating voltage at the highest required level [22]; however, it results in a great amount of power consumption. The specification on the electrode impedance of the proposed design ranges from 25 to 200 kΩ. While electrode impedance varies under a fixed stimulus current, output voltage changes correspondingly. The adaptor is used to detect output voltage every cycle of stimulation and classify electrode impedance into eight subgroups, as illustrated in figure 3. Thus, the stimulus driver can adjust $V_{CC}$ for each group of electrode impedance in the most power-saving way.

The adaptor that consists of a voltage divider and a 3-bit analog-to-digital converter (ADC) is shown on the right-hand side of figure 2. The adaptor adopts 3.3 V devices for saving the chip area. For the purpose of converting output voltage larger than $V_{DD}$ (3.3 V) into the digital code, the voltage divider is used to scale down the voltage of the output stage. The relationship between the input ($V_{stim}$) and output ($V_{feedback}$) of the voltage divider is given as follows:

$$V_{feedback} = V_{stim} \times C_3/(C_3 + C_4)\,. \quad (2)$$

In accordance with the consideration of the largest electrode impedance of 200 kΩ and stimulus current of 30 $\mu$A, the maximum convertible output voltage is 6 V, and it can be scaled down to 3.3 V by a voltage divider. Therefore, in this work, the capacitance of $C_3$ to be used is 1 pF, and the capacitance of $C_4$ is 0.82 pF.

The comparator used in the 3-bit ADC is shown in figure 4 [23]. The comparator without the dc current is very power-saving, no matter in comparing phase or holding phase. The $V_{CC}$ is conditioned in accordance with the digital output of the 3-bit ADC of the adaptor. '111' indicates the

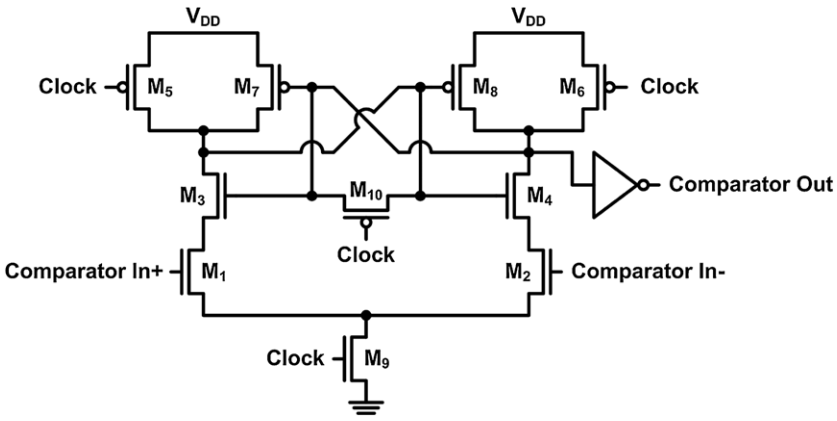


**Figure 4.** The comparator used in the 3-bit ADC of the adaptor [23].

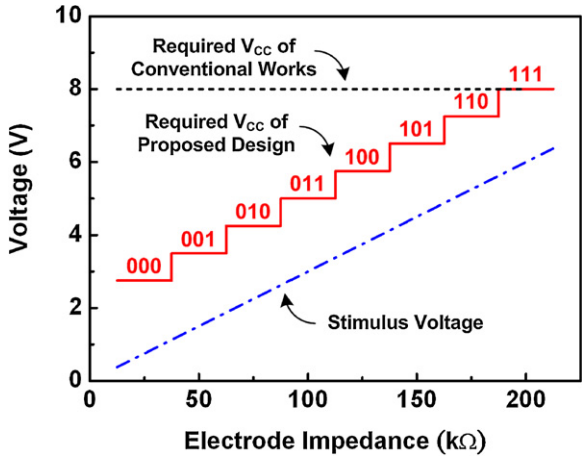


**Figure 5.** The required $V_{CC}$ of the proposed circuit and conventional works under different electrode impedances.

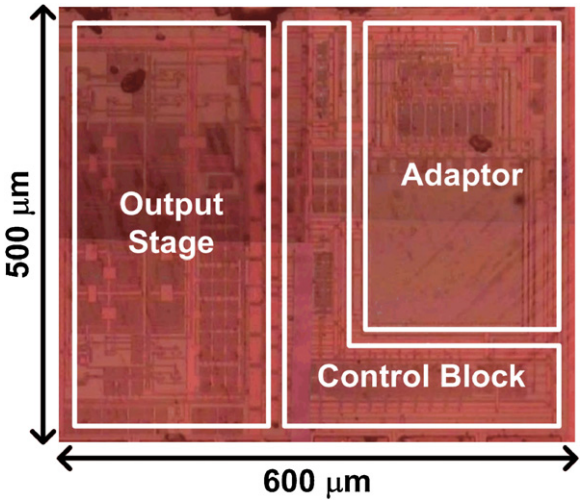


**Figure 6.** Die photo of the proposed stimulus driver with output stage, control block and adaptor, which has been fabricated in a 0.35 $\mu$m CMOS process.

highest output voltage results from the fixed stimulus current and the highest electrode impedance of specification, and then the highest $V_{CC}$ is given. '000' indicates the lowest output voltage, and then the lowest $V_{CC}$ is given. The typical voltage headroom of the stimulus driver under stimulation is 2 V and the required operating voltages ($V_{CC}$) of the proposed circuit and conventional works versus electrode impedance are compared in figure 5. Besides, the corresponding digital codes from the ADC of the proposed circuit are also provided in figure 5. While stimulation is requested, the stimulus driver delivers the first stimulus pulse. Then, the stimulus voltage and electrode impedance are known, and the digital codes are converted from the adaptor. Namely, different electrode impedances are monitored. The stimulus driver can adjust $V_{CC}$ before delivering the next stimulus pulse. The new proposed stimulus driver is provided with variable operating voltage, which can be more power efficient.

## 3. Experimental verification in silicon

The proposed stimulus driver to suppress epileptic seizure with adaptive loading design and low power consideration has been fabricated in a 0.35 $\mu$m 3.3 V/24 V CMOS process. Figure 6 shows the die photograph of the fabricated stimulus driver with the chip area of 600 × 500 $\mu$m$^2$.

Under measurement, Agilent E3631A is used to provide the fixed 3.3 V $V_{DD}$ and the adjustable $V_{CC}$. Hp 33120A is used to supply the high frequency signal for switching blocking capacitors and to enable the implanted stimulus driver. Tektronix 3054B is used to observe stimulus voltage/current of the stimulus driver. Figure 7(a) shows the measured stimulus currents passing through resistors, where 24 kΩ and 200 kΩ resistors are used to represent the equivalent electrode impedance on the simulating site. Besides, some electrodes may be modeled as a series resistor and capacitor [17]. The measured stimulus currents with 24 kΩ/200 kΩ resistors and 1 $\mu$F capacitor in series are shown in figure 7(b). The 30 $\mu$A stimulus current can be delivered after the trigger signal is sent to the driver. The turn-on time for the stimulus driver was only ∼10 $\mu$s. Figure 8 summarizes the measured stimulus currents as the electrode impedance varies from 24 to 200 kΩ. The stimulus current of the proposed design remains 30 $\mu$A constantly with varying electrode impedance. The averaged power consumption is 0.24 mW (0.56 mW) under the 24 kΩ

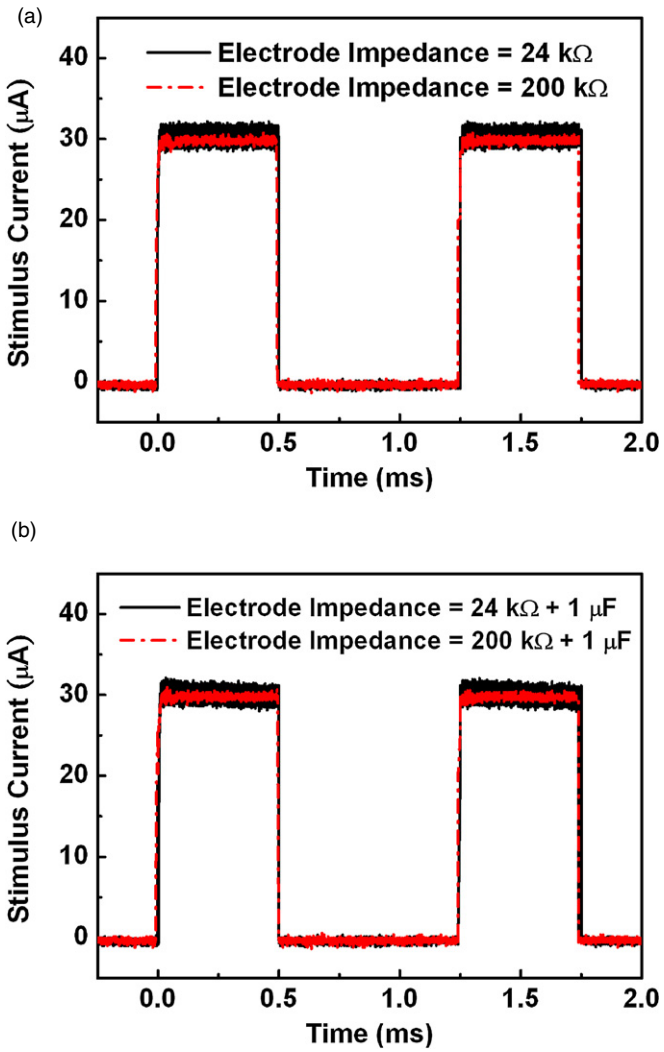


**Figure 7.** Measured stimulus currents with (a) 24 kΩ and 200 kΩ resistors, and (b) 24 kΩ and 200 kΩ resistors and 1 $\mu$F capacitor to represent electrode impedance.

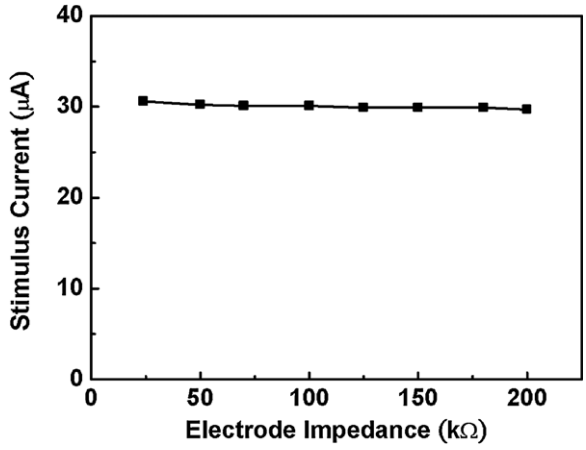


**Figure 8.** Measured stimulus currents under different electrode impedances.

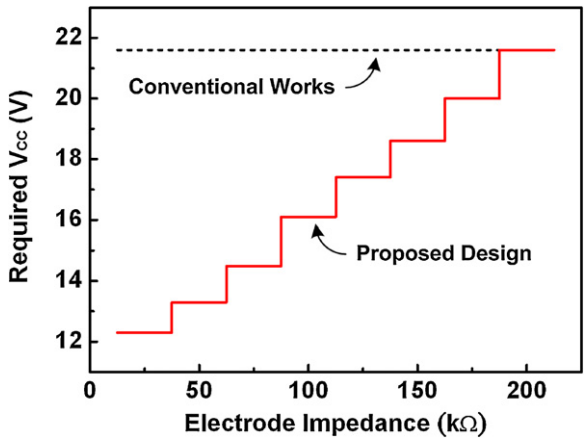


**Figure 9.** Measurement results of the required operating voltage ($V_{CC}$) under different electrode impedances.

(200 kΩ) electrode impedance. Due to the process variation in the threshold voltage of 24 V transistors, the required operating voltage ($V_{CC}$) of the proposed stimulus driver becomes higher, as shown in figure 9.

## 4. Application of the stimulus driver in an epileptic seizure monitoring and controlling system

The proposed stimulus driver was integrated into a closed-loop epileptic seizure monitoring and controlling system which was conducted by National Cheng-Kung University, Taiwan. Long-Evans rats, aged 4–6 months and weighing 500–700 g, were selected for test in this study. All surgical and experimental procedures were reviewed and approved by the Institutional Animal Care and Use Committee of National Cheng-Kung University, Taiwan. The rats were anesthetized with sodium pentobarbital (50 mg kg$^{-1}$, i.p.). By analyzing brain activities of Long-Evans rats which suffer from spontaneous absence seizures and epileptiform activities induced by pentylenetetrazol (PTZ), the system can detect epileptic seizure simultaneously and stimulate the right-side zona incerta (ZI) of Long-Evans rats. The detection electrodes were bilaterally implanted over the area of the frontal barrel cortex (anterior 2.0 mm, lateral 2.0 mm with regard to the bregma). Stimulus current is conducted by a 4-microwire bundle, each made of a Teflon-insulted stainless steel wire, to stimulate the right-side ZI (posterior 4.0 mm, lateral 2.5 mm and depth 6.7–7.2 mm). The diameter of the microwire (#7079, A-M Systems) is 50 $\mu$m. The ground electrode was implanted 2 mm caudal to lambda.

The measurement setup of the integration experiment of the proposed stimulus driver and the closed-loop epileptic seizure monitoring and controlling system are shown in figure 10. The system consists of the signal recorder, signal processor and stimulus driver [15]. In the signal recorder, the brain activities of the frontal cortex of the rat are recorded. The signal processor is used to detect the epileptic seizures with intensive and rapid brain activities. The frequency band used for EEG signal recording is 0.8–72 Hz. The time-domain and frequency-domain characteristics of EEG signals, with respect to various physiological states, were integrated as seizure detection features. A linear least-squares model

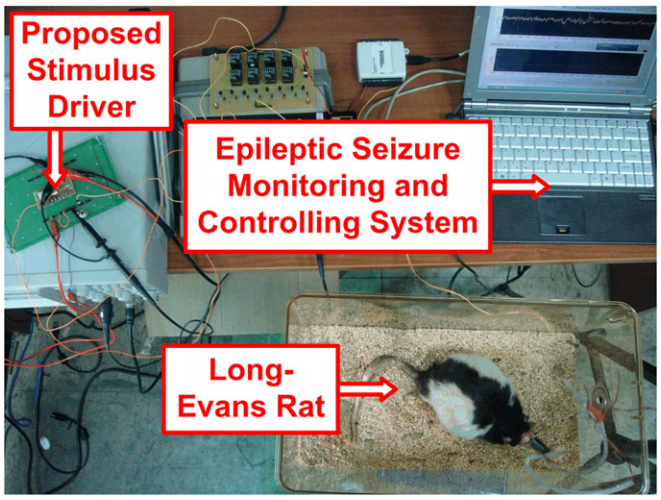


**Figure 10.** The measurement setup of the integration experiment of the proposed stimulus driver and the closed-loop epileptic seizure monitoring and controlling system.

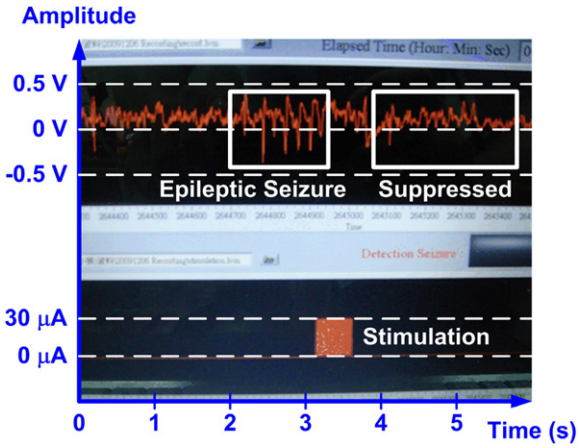


**Figure 11.** The experiment results of Long-Evans rats without injection of PTZ.

was utilized to reduce the computational cost of the seizure classifier implemented on the embedded systems. The seizure detection accuracy was greater than 92% [24]. Whenever the system detects an epileptic seizure, the proposed stimulus driver is activated by a trigger signal to stimulate ZI. The stimulus duration is set to be 0.5 s.

Two Long-Evans rats were tested. One rat was subjected to spontaneous absence seizure and the other one was subjected to PTZ-induced seizure. Each of the experiments was conducted for 10 min. Figure 11 shows one of the experimental results without injection of PTZ, the epileptic seizure of the rat with absence seizure was detected at 2 s, and the system triggered the proposed stimulus driver to stimulate ZI. After first stimulation, the intensive and rapid brain activity was suppressed. At this measurement, the electrode impedance of the Long-Evans rat was measured to be 150 kΩ, and the required $V_{CC}$ was 18 V.

The proconvulsant PTZ (20 mg kg$^{-1}$, i.p.) was injected into the other Long-Evans rat. The rat displayed intensive

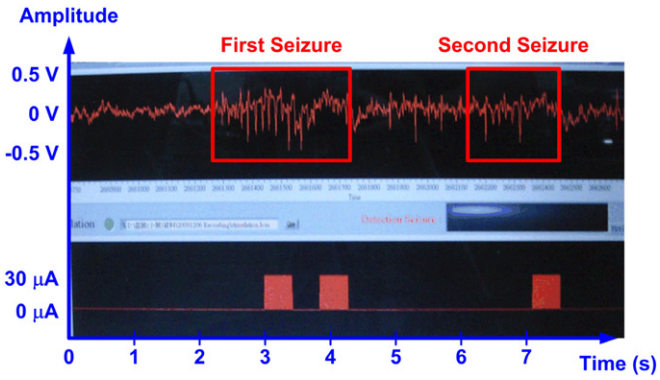


**Figure 12.** The experimental results of Long-Evans rats with injection of PTZ.

head nodding and facial twitching behavior after PTZ injection for 2 h. Figure 12 shows the experimental result with the injection of PTZ, where the abnormal brain activity was most severe. The system detected the first seizure and stimulated; however, epileptic seizure was not suppressed, and the first stimulation was invalid. Thus, abnormal brain activity was still detected by the system. The second stimulation was given to effectively suppress epileptic seizure. Because this experiment was conducted with the injection of PTZ, epileptiform activity was induced and became unstable. The second seizure just happened after the suppression of the first seizure, but it was suppressed by stimulation immediately. According to the experimental results, the functionalities of the proposed stimulus driver in the closed-loop epileptic seizure monitoring and controlling system were successfully verified.

The electrode impedance verses implanted time in different stimulus sites of right-side ZI was also measured. After the 2 h current stimulation test, the equivalent electrode impedances between two arbitrary microwires varied from 50 to 170 kΩ, which are measured by the impedance meter. Since the proposed stimulus driver can deliver the 800 Hz, 40% duty cycle and 30 $\mu$A pulse train for 0.5 s in the impedance range of 24–200 kΩ, it can be successfully integrated into the closed-loop epileptic seizure monitoring and controlling system.

## 5. Conclusion

A new stimulus driver with adaptive loading impedance and low power consideration is proposed in this work. The design has been realized in a 0.35 $\mu$m 3.3 V/24 V CMOS process to enhance the reliability under the condition of high operating voltage. In addition, the proposed stimulus driver adopts blocking capacitors to improve safety by preventing dc current flow once semiconductor failures occur. With adaptive loading consideration, the adaptor is utilized to detect and classify electrode impedance, and the output stage in the stimulus driver is able to adjust the suitable level of operating voltage. By adjustable operating voltage, the proposed stimulus driver has lower power consumption than that operated with a fixed operating voltage. According to measurement results, the stimulus current remains 30 $\mu$A while electrode impedance

varies from 24 to 200 kΩ, and the average power consumption is 0.24–0.56 mW. This design has been further integrated into the closed-loop epileptic seizure monitoring and controlling system to verify its driving ability in animal tests of Long-Evans rats.

## Acknowledgments

This work was partially supported by National Science Council (NSC), Taiwan, under contract NSC 100-2220-E-009-021, and by the 'Aim for the Top University Plan' of National Chiao-Tung University and Ministry of Education, Taiwan. The authors would like to thank Professor Fu-Zen Shaw and his research group in National Cheng-Kung University, Taiwan, for their great help with the animal test. The authors would also like to thank Professors Chung-Yu Wu, Jin-Chern Chiou, Sheng-Fu Liang, Herming Chiueh, Wen-Tai Liu and Dr Yue-Loong Hsin in Biomimetic Systems Research Center, National Chiao-Tung University, Taiwan, for their valuable suggestions during circuit design.

## References

[1] Heijbel J, Blom S and Bergfors P 1975 Benign epilepsy of children with centrotemporal EEG foci. A study of incidence rate in outpatient care *Epilepsia* **16** 657–44
[2] Cascino G 1994 Epilepsy: contemporary perspectives on evaluation and treatment *Proc. Mayo Clin.* **69** 1199–211
[3] Baker G, Jacoby A, Buck D, Stalgis C and Monnet D 1997 Quality of life of people with epilepsy: a European study *Epilepsia* **38** 353–62
[4] Litt B, Alessandro M, Esteller R, Echauz J and Vachtsevanos G 2003 Translating seizure detection, prediction and brain stimulation into implantable devices for epilepsy *Proc. IEEE EMBS Conf. on Neural Engineering* pp 485–8
[5] Cantor S and Cantor S 1995 Physiological description of the neuron and the human nervous system *Proc. IEEE Int. Frequency Control Symp.* pp 3–9
[6] Sivaprakasam M, Liu W, Humayun M and Weiland J 2005 A variable range bi-phasic current stimulus driver circuitry for an implantable retinal prosthetic device *IEEE J. Solid-State Circuits* **40** 763–71
[7] Dommel N, Wong Y, Lehmann T, Dodds C, Lovell N and Suaning G 2009 A CMOS retinal neurostimulator capable of focussed, simultaneous stimulation *J. Neural Eng.* **6** 035006
[8] Theodore W and Fisher R 2004 Brain stimulation for epilepsy *Lancet Neurol.* **3** 111–8
[9] Stacey W and Litt B 2008 Technology insight: neuroengineering and epilepsy—designing devices for seizure control *Nat. Clin. Pract. Neurol.* **4** 190–201
[10] Iasemidis L 2003 Epileptic seizure prediction and control *IEEE Trans. Biomed. Eng.* **50** 549–58
[11] Mormann F, Andrzejak R, Elger C and Lehnertz K 2007 Seizure prediction: the long and winding road *Brain* **130** 314–33
[12] Adeli H, Ghosh-Dastidar S and Dadmehr N 2007 A wavelet-chaos methodology for analysis of EEGs and EEG subbands to detect seizure and epilepsy *IEEE Trans. Biomed. Eng.* **54** 205–11
[13] Gui H, Xia Y, Liu F, Liu X, Dai S, Lei L and Wang Y 2009 Based on the time–frequency analysis to distinguish different epileptiform EEG signals *Proc. Int. Conf. on Bioinformatics and Biomedical Engineering* pp 1–3
[14] Asfour A, Fiche C and Deransart C 2007 Dedicated electronics for electrical stimulation and EEG recording using the same electrodes: application to the automatic control of epileptic seizures by neuro-stimulation *Proc. Instrumentation and Measurement Technology Conf.* pp 1–4
[15] Young C, Liang S, Chang D, Liao Y, Shaw F and Hsieh C 2010 A portable wireless online closed-loop seizure controller in freely moving rats *IEEE Trans. Instrum. Meas.* **60** 513–21
[16] Tsai H and Ker M 2010 Design of 2xVDD-tolerant mixed-voltage I/O buffer against gate-oxide reliability and hot-carrier degradation *Microelectron. Reliab.* **50** 48–56
[17] Kelly S and Wyatt J 2011 A power-efficient neural tissue stimulator with energy recovery *IEEE Trans. Biomed. Circuits Syst.* **5** 20–9
[18] Halpern M and Fallon J 2010 Current waveforms for neural stimulation-charge delivery with reduced maximum electrode voltage *IEEE Trans. Biomed. Eng.* **57** 2304–12
[19] Ker M, Chen W, Lin C and Weng Y 2010 Circuit design of stimulus driver for adaptive loading applications *Proc. Neural Interfaces Conf.* p 125
[20] Brindley G 1995 The first 500 sacral anterior root stimulators: implant failures and their repair *Paraplegia* **33** 5–9
[21] Liu X, Demosthenous A and Donaldson N 2008 An integrated implantable stimulator that is fail-safe without off-chip blocking-capacitors *IEEE Trans. Biomed. Circuits Syst.* **2** 231–44
[22] Ghovanloo M and Najafi K 2005 A compact large voltage-compliance high output-impedance programmable current source for implantable microstimulators *IEEE Trans. Biomed. Eng.* **52** 97–105
[23] Chang Y, Wang C and Wang C 2007 A 8-bit 500-KS/s low power SAR ADC for bio-medical application *Proc. IEEE Asian Solid-State Circuits Conf.* pp 228–31
[24] Liang S, Shaw F, Young C, Chang D and Liao Y 2010 A closed-loop brain computer interface for real-time seizure detection and control *Proc. IEEE EMBS Conf.* pp 4950–3